Research Article

Peng Zhang, Xuemei Zhang, Yamin Zhang, Yuanxun Zheng*, and Tingya Wang

Gray correlation analysis of factors influencing compressive strength and durability of nano-SiO_2 and PVA fiber reinforced geopolymer mortar

https://doi.org/10.1515/ntrev-2022-0493
received April 23, 2022; accepted October 18, 2022

Abstract: To investigate the mechanical properties and durability of nano-SiO_2, polyvinyl alcohol (PVA) fiber-modified fly ash (FA), and metakaolin (MK)-based geopolymer mortar (FMGM), tests of compressive strength, electrical flux, freeze–thaw cycles, and sulfate dry and wet cycles were conducted. Based on the experimental results, combined with Dunn's gray correlation theory analysis method, a mathematical analysis of the effect sensitivity of the contents of the four mixtures on the mechanical properties and durability of FMGM was carried out. The method of gray correlation analysis can solve the mathematical problem with partial unclear and uncertain information, and the method requires less data and less computation compared with other mathematical analysis method. The results showed that the gray correlation degree between the content of MK and the electric flux value is higher than the that of other comparison sequence and each reference sequence, while the gray correlation degree between the PVA fiber dosage and the loss rate of compressive strength is lower than that of other comparison sequence and each reference sequence. The influence of the four mixture contents on the compressive strength and mass loss rate was in the following decreasing order: MK and FA, PVA fiber, and nano-SiO_2. In addition, the influence of the four material mixture contents on the electric flux value and compressive strength loss rate was consistent in the following decreasing order: MK and FA, nano-SiO_2, and PVA fiber. Furthermore, the mechanical properties and durability reached the optimum when the PVA fiber content was 0.6% and the dosage of nano-SiO_2 was 1.0%. The results of this study can provide a new method for the analysis and evaluation of mechanical properties and durability of nano-SiO_2 and PVA fiber-reinforced FMGM in future.

Keywords: gray correlation, geopolymer mortar, mechanical properties, durability

1 Introduction

Since the reform and opening up, due to rapid economic development, China has emerged as a major energy-producing and consuming country, and its carbon emissions have been the highest in the world. Despite the global economy being affected by the epidemic in 2020, the total global carbon emissions remained high, reaching 32.28 billion tons, with China accounting for the highest share (30.7%). The cement industry is currently the second-largest industry in terms of carbon emissions, behind only the steel industry, and the production of cement mortar or concrete releases large amounts of carbon dioxide into the environment [1,2]. This is a serious violation of China's policy of "double carbon" peaking by 2030, and carbon neutrality by 2060. It has been reported that each ton of cement production consumes nearly 100 kg of standard coal and emits approximately 1,000 kg of carbon dioxide; therefore, the massive use of cement will lead to increasingly serious problems of resource consumption, energy waste, and environmental pollution [3]. Traditional cement-based composites have disadvantages such as easy cracking, poor durability, low strength, and insufficient water retention [4,5]. Therefore, the development of a green and environmentally friendly cementitious material that can be used as an alternative to cement has become an urgent need [6,7].

Geopolymers are a class of new non-metallic material, proposed by Professor Davidovits in 1978, with inorganic

* **Corresponding author: Yuanxun Zheng,** School of Water Conservancy Engineering, Zhengzhou University, Zhengzhou, 450001, China, e-mail: yxzheng@zzu.edu.cn
Peng Zhang: School of Water Conservancy Engineering, Zhengzhou University, Zhengzhou, 450001, China; Yellow River Laboratory, Zhengzhou University, Zhengzhou, 450001, China
Xuemei Zhang, Tingya Wang: School of Water Conservancy Engineering, Zhengzhou University, Zhengzhou, 450001, China
Yamin Zhang: Library, Zhengzhou University, Zhengzhou, 450001, China

SiO_2 and AlO_4 tetrahedra as the main composition. Geopolymers represent a new calcium-free aluminum-silica cementitious material with a three-dimensional shelf-like structure [8]. Compared with traditional silicate cement and concrete, a geopolymer has better workability, mechanical properties [9,10], and durability [11,12]. Geopolymers are environment friendly as their preparation process does not require the "two grinding and one burning" process [13], which saves a considerable amount of resources and energy and prevents NO_X, SO_X, and CO generation and substantial CO_2 emissions [14]. In addition, geopolymer materials have advantages such as fast hardening, high early strength, low shrinkage, low permeability, high-temperature resistance, good thermal insulation, and adjustable thermal expansion coefficient [15]. Geopolymers have higher strength, lower water absorption, and lower porosity than ordinary silicate cement [16]. Chithambaram *et al.* [15] studied the thermodynamic properties of geopolymer mortar manufactured using slag powder instead of fly ash (FA) and found that geopolymer mortar exhibits a dense structure, early curing, and increased strength. Sreevidya *et al.* [17] studied the strength of FA geopolymer mortar and found that the highest 28 days compressive strength of the specimens was obtained when the exciter/FA mass ratio was 0.416. Bingol *et al.* [18] studied the durability of alkali-activated slag geopolymer mortar and found that the corrosion resistance of alkali-activated slag geopolymer mortar in corrosive media was significantly higher than that of cement mortar. Geopolymer mortars, given their excellent characteristics, have broad application prospects in the construction of roads and bridges, water conservancy, and other fields [19].

The drawbacks of brittleness, low toughness, and low deformation resistance exhibited by both geopolymer and cement mortars can be mitigated by adding certain high-performance fibers to geopolymer mortars [20]. The fiber materials [21] commonly used in mortars are polypropylene alcohol fibers [22,23], steel fibers [24,25], glass fibers [26], polyvinyl alcohol (PVA) fibers [27,28], *etc.* PVA fibers exhibit high tensile strength and modulus of elasticity, good adhesion with cementitious materials, good hydrophilicity, and nontoxicity. In addition, PVA fibers exhibit good acid and alkali resistance, which can improve the durability of the material [29]. Du and Li [30] showed that PVA fiber-reinforced high-strength concrete has excellent mechanical properties. Wang *et al.* [31] showed that the durability and ductility of rubber concrete improves with PVA-fiber reinforcement. PVA fiber incorporated into geopolymer mortars can improve the toughness of the material [32], changing the damage mode of the material from brittle to ductile [33]. Therefore, the use of PVA fibers in geopolymer mortars improves their properties, making them suitable for many applications [34].

Nanomaterials are favored by scholars all over the world because of their small-size effect, quantum effect, and interfacial effect, which can enhance traditional construction materials in terms of their structure and physicochemical properties. Nano-SiO_2 has many advantages, such as being non-toxic, odorless, and non-polluting, in addition to having a small particle size. The application of nanomaterials in mortars or concretes can play the role of nano-filling and nano-enhancement, improve the performance of the interfacial transition zone in mortar, optimize the microstructure of mortar, and reduce the porosity while enhancing the impermeability [35], mechanical properties [36,37], and durability [38,39] of the matrix. With the maturity of nano-SiO_2 modification technology for cement-based materials, many scholars have studied the properties of nano-SiO_2 incorporated into geopolymer-based construction materials. Li [40] studied high-strength concrete with bulk FA mixed with nano-SiO_2 and found that it exhibited increased compressive strength and improved pore distribution compared to concrete without nano-SiO_2. Xiao *et al.* [41] studied the effect of nano-SiO_2 on different microstructures and impermeability of graded concrete and found that the microstructure was the densest and the impermeability was the strongest when the Fuller exponent was 0.4–1.0. Related studies have shown that the incorporation of an appropriate quantity of nano-SiO_2 in geopolymer mortar can improve its microstructure and durability properties such as frost resistance, permeability resistance, acid rain erosion line, and washout resistance, as well as increase the strength of the geopolymer mortar [42].

Environmental differences between regions and harsh environments have caused serious damage to exposed buildings, such as impact, abrasion, carbonization, freeze–thaw damage, and salt–freeze damage. These damages directly or indirectly cause cracks, corrosion, decline in load-bearing capacity and durability, and other effects. Offshore projects and structures are subjected to damage owing to harsh marine environment [43–46]. Many buildings have suffered freeze–thaw damage due to the existence of large cold zones, especially in the north [47]. The degradation of building materials due to freeze–thaw cycles is an important durability issue for cementitious materials and structures in cold regions [48]. Severely cold places have a high demand for geopolymer mortars as repair and reinforcement materials [49]. Owing to their excellent durability, geopolymer mortars are more energy efficient than cement-based materials, and the incorporation of nano-SiO_2 and PVA fibers can enhance the toughness of the matrix and durability of the material [50–53].

Therefore, it is necessary to study the mechanical properties and durability of geopolymer mortars incorporated with nano-SiO_2 and PVA fibers and reveal the mechanism of nano-SiO_2 and PVA fibers that enhance the mechanical properties and durability of geopolymer mortars.

There are many ways to analyze the experimental data involving the mechanical properties and durability parameters of nano-SiO_2, PVA fiber-reinforced FA, and metakaolin (MK)-based geopolymer mortar (FMGM). Most conventional methods of system analysis are traditional mathematical and statistical analyses, including regression analysis [54], analysis of variance [55], and principal component analysis [56]. Among these, regression analysis is the most widely used. Its types include linear, multi-factor, single-factor, stepwise, and non-stepwise. Regression is best suited in the case of a small number of variables, with a large amount of statistical data that exhibit typical distribution patterns, such as linear, exponential, logarithmic, and normal distributions. The results are not intuitive when the amount of information is insufficient. However, for experiments on the mechanical properties and durability of nano-SiO_2 and PVA fiber-reinforced FMGM, there are certain limitations on the acquisition of experimental data. (1) It is difficult to obtain a large amount of valid data under exactly the same experimental conditions due to the influence of human and environmental factors. (2) It is difficult to maintain a certain distribution pattern of experimental data [57]. For such data, if traditional mathematical and statistical analysis methods are used, it is likely that the system is found unsolvable, or that the conclusion deviates from the facts and is misleading.

Gray correlation analysis is an important method of the gray system theory [58,59] that requires less data and computation [60–62]. Gray correlation analysis theory has been widely used in the evaluation and analysis of various properties of concrete [63–66]. Lai *et al.* [67] evaluated concrete structure crack patterns and found that the Mahalanobis distance and gray correlation analysis can effectively classify the dataset and identify the concrete resultant crack types. Arici and Kelestemur [68] used the Taguchi theory-based gray correlation analysis method to obtain the optimal parameter classes that satisfy the mortar performance. With the exploration of social development, the economy, and other abstract systems, gray correlation theory is gradually being improved and has been widely used in the analysis of water resources, the economy, agriculture, and other fields. Gray correlation theory has now become a new theoretical tool for the analysis, modeling, prediction, decision making, control, and transformation of objective systems. Gray correlation analysis can not only compensate for the shortcomings of conventional system analysis methods but also has the advantages of a simple calculation process, small calculation volume, and intuitive results that are suitable for practical engineering applications. Therefore, in this study, using the method of gray correlation analysis, comparison and reference sequences were established to calculate the weight ranking for the influence of the four mixture contents on the mechanical properties and durability evaluation indices of FMGM. The quantities of alkali exciter, FA, water reducer, MK, water, quartz sand, PVA fiber, and nano-SiO_2 were used as the comparison sequence. The electric flux value, compressive strength loss rate, mass loss rate index under sulfate attack, and compressive strength of the material were used as the reference sequence. Based on the calculation results, the effect sensitivity of the contents of the four mixtures on the mechanical properties and durability of FMGM was analyzed.

2 Experimental procedure

2.1 Raw materials and mix design

In this study, a control variable method was chosen in the mix design, that is, the water–cement ratio, cement–sand ratio, water–glass modulus, and admixture were fixed, while the admixture of nano-SiO_2 or PVA fiber was changed. The water–cement ratio (the ratio of water to cementitious material mass contained in the water and alkali exciter) was 0.65, and the cement–sand ratio was 1:1. FA, in the same amount, was used to replace 30% of the kaolinite mass, and the alkali exciter solution was prepared by mixing sodium hydroxide, water glass, and water. The content of Na_2O is 8.2%, and the content of SiO_2 is 26.1% in water glass. The water glass has the gravity of 1.38 g/cm^3 and solid content of 34.4%. The initial modulus of the water glass was 3.2, which was adjusted to 1.3 by adding sodium hydroxide flakes, and then, the mass fraction of sodium oxide in the solution was adjusted to 15% by adding water. The concentration of the NaOH is 99.0%. The chemical and physical composition of kaolinite is listed in Tables 1 and 2. The primary FA used was produced by Datang Luoyang Thermal Power Co., Ltd.

Table 1: Chemical composition of MK

Chemical composition	SiO_2	Al_2O_3	Fe_2O_3	CaO + MgO	K_2O + Na_2O
Content (%)	54 ± 2	43 ± 2	≤1.3	≤0.8	≤0.7

Table 2: Physical properties of MK

Whiteness (%)	Activity index (%)	Availability of lime (mL/4N-HCl)	Average particle size (μm)	Ignition loss (%)
75	12	1,350	1.2	0.5

Table 3: Chemical compositions of FA

Chemical compositions (wt%)	SiO_2	Al_2O_3	Fe_2O_3	CaO + MgO	SO_3
FA	60.98	24.47	6.70	5.58	0.27

The main chemical and physical properties of the FA are listed in Tables 3 and 4. The quartz sand used was of extra-fine quality from the Gongyi Yuanheng Water Purification Material Plant, with a particle size range of 75–120 μm. The modulus of the sodium silicate solution used in the test was 3.2, the specific gravity was 1.38 g/cm^3, the solid content was 34.3%, and the purity of sodium hydroxide was 99.0%. The PVA fibers were produced by Kuraray Co., Ltd. The apparent density of nano-SiO_2 was 54 g/L, pH was 6.21, average particle size was 30 nm, heating reduction and cautery reduction were 1.0%, specific surface area was 200 m^2/g, and content was 99.7%. The water-reducing agent had a water reduction rate of 21%, pH value of 4.52, fixed content of 24.56%, and density of 1.058 g/cm^3. The volume doping of the PVA fibers used in this study was in the range of 0–1.2%, varied in increments of 0.2%. The nano-SiO_2 contents were varied in the range of 0–2.5%, in increments of 0.5%. The nano-SiO_2 content was determined as the ratio of the amount of nano-SiO_2 to the amount of MK and FA.

2.2 Preparation of mixture

During the mixing procedure of geopolymer mortar, the precursor was first dry mixed with quartz sand for 2 min. The sand was spread on a plate and dried in an oven at 70°C for 24 h prior to mixing. After that, both PVA fiber and nano-SiO_2 (NS) was added to the mixer in 2 batches, stirring for 2 min each time. Then, the mixed solution of alkaline solution and super plasticizer was added to the dry mixture. The prepared alkaline solution should be set for 1 day before use. After thoroughly mixing, the fresh mortar was molded. In this study, 22 groups of specimens with different nano-SiO_2 and PVA fiber content were tested. The molded specimens were cured in ambient environment (about 28°C) for 24 h and then transferred to a curing room (20 ± 2°C, 95% humidity) for 28 days.

2.3 Experimental method

The durability of nano-SiO_2 and PVA-fiber-reinforced FMGM was investigated, and the compressive strength was tested using a uniaxial compressive test. The electric flux was tested using a chloride ion electric flux test. The cathode was connected to a 3.0% NaCl solution, and the anode was connected to a 0.3 M NaOH solution. 60 V DC voltage was continuously supplied for 6 h, and the current was recorded every 30 min. The average value of triplicate samples was recorded as final. The apparent damage to the geopolymer mortar was observed by rapid freeze–thaw tests after 25 freeze–thaw cycles for each doping amount. After 26 days of standard curing, the samples were immersed in 15–20°C water for 2 days and then were surface dried. The single freezing–thawing time was 8 h (freezing for 4 h and thawing for 4 h). The temperature of sample was controlled at −17 and 8°C at the end of freezing and thawing, respectively. After 26 days of standard curing, the samples were put in an oven of 80 ± 5°C for 48 h and then were cooled to room temperature in a dry environment. The dried samples were placed at intervals in the testing machine. The 5% Na_2SO_4 was used as the erosion solution, and the solution was replaced by fresh solution every month. The compressive strength loss coefficient of the geopolymer mortar was tested for each admixture, and the quality change rate of the geopolymer mortar was tested after 90 dry and wet cycles of sulfate, *via* the sulfate dry and wet cycle tests. Therefore, in the gray correlation analysis, the compressive strength, electric flux value, mass loss rate, and compressive strength loss rate were selected as the reference sequence, and the ratio design of each material of the

Table 4: Physical properties of FA

Water absorbing capacity (%)	Standard consistency (%)	Bulk density (g/cm^3)	Specific gravity (g/cm^3)
105	47.1	0.77	2.16

geopolymer mortar was used as the comparison sequence. However, because the dosage amounts of water, quartz sand, water glass, sodium hydroxide, and water-reducing agent were fixed values, only the dosages of partial kaolin, FA, PVA fiber, and nano-SiO_2 were chosen as the comparison sequence.

2.4 The experimental result

The mix proportions of the nano-SiO_2 and PVA fiber-reinforced FMGM are listed in Table 5. The values of each comparative sequence are listed in Table 6.

3 Model establishment

3.1 Brief description of gray correlation theory

Gray correlation theory is a system science theory pioneered by a famous scholar in China. Professor Deng [70–72] proposed the gray correlation model and the concept of gray correlation degree analysis for each subsystem to establish a relationship between the system and each subsystem (influencing factors). However, statistical data in China are very limited, and some data are incomplete. Human influence factors are inevitable, so it is common for the data to have many inaccuracies. It may be difficult to find a suitable distribution pattern, making data processing and analysis difficult.

At present, the more commonly used methods are gray correlation, regression analysis, and so on. Although regression analysis can predict and work out the corresponding function, and carry out residual test on the results, it requires a large number of samples and is limited in some conditions, so it can only be used for prediction. Gray correlation analysis requires fewer samples, which can be used for prediction and analysis. Therefore, gray correlation analysis can compensate for the shortcomings of traditional mathematical and statistical methods and has become a widely used system analysis method. The specific steps for conducting the gray correlation analysis are explained below.

3.2 Establishment of the gray correlation model

3.2.1 Determination of the sequence of system analysis

The series for conducting system analysis include the parent series, which represents the system, and the subseries, which represents the subsystem.

Table 5: Mixing proportions of nano-SiO_2 and PVA fiber reinforced FMGM [69]&&&

Mix no.	Water (kg/m^3)	MK (kg/m^3)	FA (kg/m^3)	Quartz sand (kg/m^3)	Water glass (kg/m^3)	NaOH (kg/m^3)	PVA fiber (%)	NS (%)	Water-reducing agents (kg/m^3)
1	106.2	429.5	184.1	613.6	445.4	71	0	0	3.07
2	106.2	429.5	184.1	613.6	445.4	71	0.2	0	3.07
3	106.2	429.5	184.1	613.6	445.4	71	0.4	0	3.07
4	106.2	429.5	184.1	613.6	445.4	71	0.6	0	3.07
5	106.2	429.5	184.1	613.6	445.4	71	0.8	0	3.07
6	106.2	429.5	184.1	613.6	445.4	71	1.0	0	3.07
7	106.2	429.5	184.1	613.6	445.4	71	1.2	0	3.07
8	106.2	427.2	183.1	613.6	445.4	71	0	0.5	3.07
9	106.2	425.0	182.2	613.6	445.4	71	0	1.0	3.07
10	106.2	422.7	181.2	613.6	445.4	71	0	1.5	3.07
11	106.2	420.4	180.2	613.6	445.4	71	0	2.0	3.07
12	106.2	418.1	179.2	613.6	445.4	71	0	2.5	3.07
13	106.2	425.0	182.2	613.6	445.4	71	0.2	1.0	3.07
14	106.2	425.0	182.2	613.6	445.4	71	0.4	1.0	3.07
15	106.2	425.0	182.2	613.6	445.4	71	0.8	1.0	3.07
16	106.2	425.0	182.2	613.6	445.4	71	1.0	1.0	3.07
17	106.2	425.0	182.2	613.6	445.4	71	1.2	1.0	3.07
18	106.2	427.2	183.1	613.6	445.4	71	0.6	0.5	3.07
19	106.2	425.0	182.2	613.6	445.4	71	0.6	1.0	3.07
20	106.2	422.7	181.2	613.6	445.4	71	0.6	1.5	3.07
21	106.2	420.4	180.2	613.6	445.4	71	0.6	2.0	3.07
22	106.2	418.1	179.2	613.6	445.4	71	0.6	2.5	3.07

Table 6: Reference sequence of nano-SiO_2 and PVA fiber reinforced FMGM

Mix no.	Compressive strength (MPa)	Electric flux values (C)	Loss rate of compressive strength (%)	Mass loss rate (%)
1	44.2	1426.31	18.8	−3.74
2	50.8	1294.38	17.7	2.75
3	55.3	1216.08	15.9	2.46
4	58.5	1185.84	14.7	1.81
5	60.3	1150.24	12.6	1.44
6	50.5	1158.52	10.1	1.64
7	48.1	1195.41	8.9	2.07
8	45.0	1220.82	17.1	−2.31
9	47.3	1185.06	15.0	−1.12
10	50.1	1121.13	12.4	1.6
11	48.8	1164.84	13.5	2.1
12	46.4	1190.52	15.7	1.9
13	53.9	1147.62	13.7	2.06
14	57.4	1107.48	11.1	1.47
15	62.4	1071.78	8.2	0.82
16	55.7	1076.94	6.8	0.99
17	54.1	1102.36	5.4	1.38
18	59.1	1157.88	11.2	1.67
19	61.1	1096.02	9.7	1.21
20	63.6	1055.16	7.5	0.92
21	62.3	1107.06	11.6	1.15
22	59.7	1166.98	14.4	1.49

1) Determination of the parent series. The parent series, also known as the main series, reference series, or parent indicator, is a data series that can reflect the characteristics of the system behavior and is denoted as X_0.

$$X_0 = \{x_0(1), x_0(2),\ldots,x_0(n)\}. \tag{1}$$

2) Determination of the sub-series. Known as the correlation series, comparison series, or sub-indicator, it is a data series consisting of various factors that affect the behavior of the system and is denoted as X_i, i = 1,2,3...n.

$$\begin{cases} X_1 = \{x_1(1), x_1(2),\ldots,x_1(n)\} \\ \vdots \\ X_i = \{x_i(1), x_i(2),\ldots,x_i(n)\} \\ \vdots \\ X_m = \{x_m(1), x_m(2),\ldots,x_m(n)\}. \end{cases} \tag{2}$$

3) Determination of the systematic series for gray correlation analysis is as follows:

$$\{X_0, X_1,\ldots,X_i,\ldots,X_m\}.$$

3.2.2 Preprocessing of variables

1) The mean of each indicator is determined as follows:

$$\overline{x_i} = \frac{1}{n}(x_i(1) + x_i(2)+\ldots+x_i(n)). \tag{3}$$

2) Each element of the indicator is divided by the mean, and the series is normalized to obtain a new data column, $x_i(k)$.

$$x_i(k) = \frac{x_i(k)}{\overline{x_i}},\ k = 1, 2,\ldots, m;\quad i = 0, 1,\ldots n. \tag{4}$$

It is necessary to preprocess the variables and narrow the range of variables to simplify the calculation.

3.2.3 Calculation of the correlation coefficient

1) The minimum and maximum differences between the two levels are calculated as follows:

$$a = \min_i \min_k |x_0(k) - x_i(k)|,\quad i = 0, 1,\ldots, n, \tag{5}$$

$$b = \min_i \max_k |x_0(k) - x_i(k)|,\quad k = 1, 2,\ldots, m, \tag{6}$$

where a and b are the minimum and maximum differences between the two levels, respectively.

2) The gray correlation coefficient of the evaluation object is calculated as follows:

$$\gamma_i(x_0(k), x_i(k)) = \frac{a + \rho b}{|x_0(k) - x_i(k)| + \rho b}, \tag{7}$$

where $\gamma_i(k)$ is the gray correlation coefficient between $x_0(k)$ and $x_i(k)$; $\rho \in (0, 1)$, where ρ represents the resolution coefficient, often taken as 0.5, and its value is negatively correlated with the resolution ability, that is, the larger the resolution coefficient, the smaller the resolution ability of the evaluation scheme.

3.2.4 Calculation of gray correlation

The gray correlation coefficient between X_0 and $X_i(i = 1, 2, \ldots n)$ can be calculated as follows:

$$\eta_i(X_0, X_i) = \frac{1}{n}\sum_{k=1}^{n}\gamma_i(x_0(k), x_i(k)),\ k = 1, 2,\ldots,n, \tag{8}$$

where, $\eta_i(X_0, X_i)$ is the gray correlation coefficient between X_0 and $X_i(i = 1, 2, \ldots n)$.

3.2.5 Gray relational decision

According to the above operation steps, the gray correlation degree of each subsequence with the parent sequence can be determined and then compared in terms of size. The greater the gray correlation, the greater is the influence on the parent index.

4 Model training and result analysis

In order to analyze the effects of different factors on the durability of the nano-SiO_2 and PVA fiber reinforced FMGM, a gray correlation was performed with FA admixture, MK admixture, PVA fiber admixture, and SiO_2 nanoparticle admixture as the comparison sequence and the mass loss rate, electric flux value, compressive strength loss rate, and compressive strength of the FMGM as the reference sequence.

The variables were first preprocessed, that is, the variables were made dimensionless, and the preprocessed results are listed in Table 7.

The correlation coefficients of the FA admixture, MK admixture, PVA fiber admixture, nano-SiO_2 admixture, mass loss rate, electric flux value, compressive strength loss rate, and compressive strength of nano-SiO_2 and PVA fiber-reinforced FMGM were calculated and the results are displayed in Figures 1–4.

In Figures 1–4, most of the correlation curves of MK and FA are in a state of coincidence. By calculating the correlation coefficients of FA dosing, MK dosing, PVA fiber dosing, and nano-SiO_2 dosing with the mass loss rate, electric flux value, compressive strength loss rate, and compressive strength of the nano-SiO_2 and PVA fiber-reinforced FMGM under different ratio designs, it can be seen that the correlation coefficients of PVA fiber dosing first increased and then decreased when the nano-SiO_2 dosage was kept constant using the control variable method. The correlation coefficient of the nano-SiO_2 dosage also tends to increase and then decrease when the PVA fiber dosage is constant. At the same time, the correlation coefficient of PVA fiber doping is higher when the PVA fiber doping is 0.6%, and the correlation coefficient of nano-SiO_2 doping is higher when the nano-SiO_2 doping is 1.0%. From Tables 6–9, it can be seen that the correlation coefficients of nano-SiO_2 and PVA fiber doping vary widely, and the mass loss rate, electric flux value, compressive strength

Table 7: Pre-processed data of each factor

Mix no.	MK	FA	PVA fiber	NS	Compressive strength	Electric flux values	Loss rate of compressive strength	Mass loss rate
1	1.0097	1.0096	0.0000	0.0000	0.8140	1.2258	1.5375	−3.4630
2	1.0097	1.0096	0.4074	0.0000	0.9355	1.1124	1.4476	2.5463
3	1.0097	1.0096	0.8148	0.0000	1.0184	1.0451	1.3304	2.2778
4	1.0097	1.0096	1.2222	0.0000	1.0773	1.0191	1.2022	1.6759
5	1.0097	1.0096	1.6296	0.0000	1.1105	0.9885	1.0305	1.3333
6	1.0097	1.0096	2.0370	0.0000	0.9300	0.9957	0.8260	1.5185
7	1.0097	1.0096	2.4444	0.0000	0.8858	1.0274	0.7279	1.9167
8	1.0043	1.0042	0.0000	0.5500	0.8287	1.0492	1.3985	−2.1389
9	0.9991	0.9992	0.0000	1.1000	0.8711	1.0185	1.2268	−1.037
10	0.9937	0.9937	0.0000	1.6500	0.9227	0.9635	1.0141	1.4815
11	0.9883	0.9883	0.0000	2.2000	0.8987	1.0011	1.1041	1.9444
12	0.9829	0.9828	0.0000	2.7500	0.8545	1.0232	1.2840	1.7593
13	0.9991	0.9992	0.4074	1.1000	0.9926	0.9863	1.1204	1.9074
14	0.9991	0.9992	0.8148	1.1000	1.0571	0.9518	0.9807	1.3611
15	0.9991	0.9992	1.6296	1.1000	1.1492	0.9211	0.6706	0.7593
16	0.9991	0.9992	2.0370	1.1000	1.0258	0.9256	0.5561	0.9167
17	0.9991	0.9992	2.4444	1.1000	0.9963	0.9474	0.4416	1.2778
18	1.0043	1.0042	1.2222	0.5500	1.0884	0.9951	0.9160	1.5463
19	0.9991	0.9992	1.2222	1.1000	1.1252	0.9419	0.7933	1.1204
20	0.9937	0.9937	1.2222	1.6500	1.1713	0.9068	0.6134	0.8519
21	0.9883	0.9883	1.2222	2.2000	1.1473	0.9514	0.9487	1.0648
22	0.9829	0.9828	1.2222	2.7500	1.0994	1.0029	0.9323	1.3769

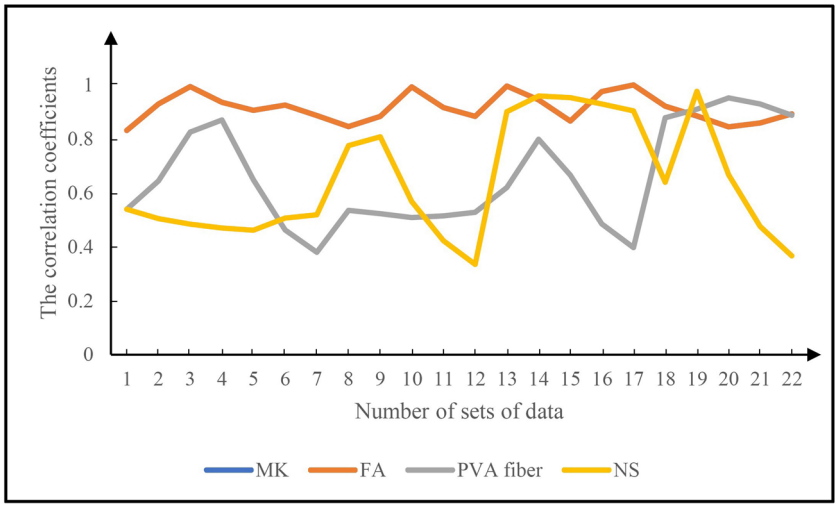

Figure 1: Correlation between various factors and compressive strength.

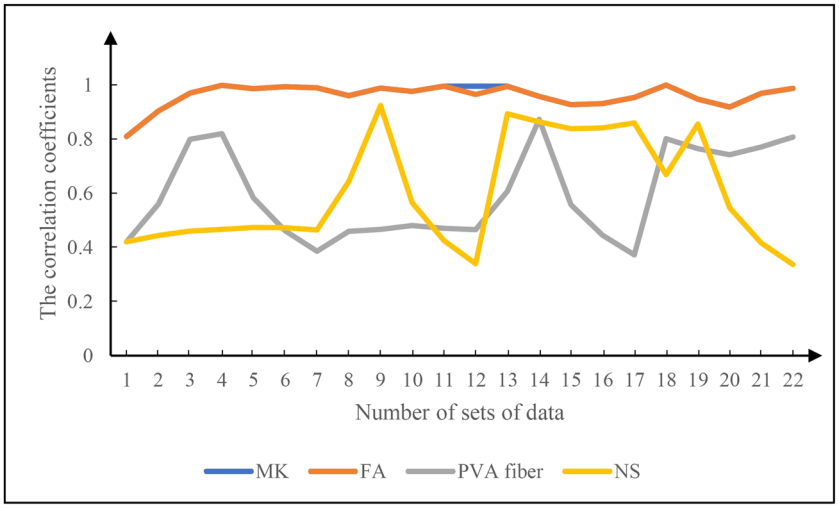

Figure 2: Correlation between each factor and electric flux value.

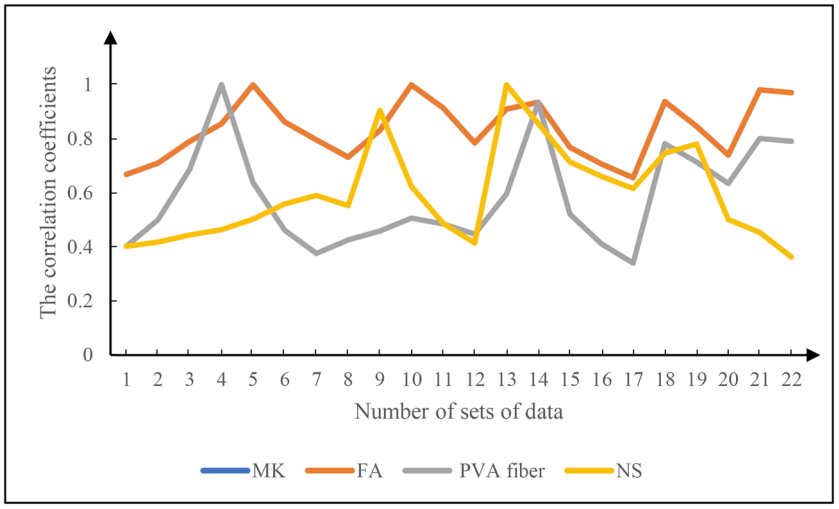

Figure 3: Correlation between various factors and loss rate of compressive strength.

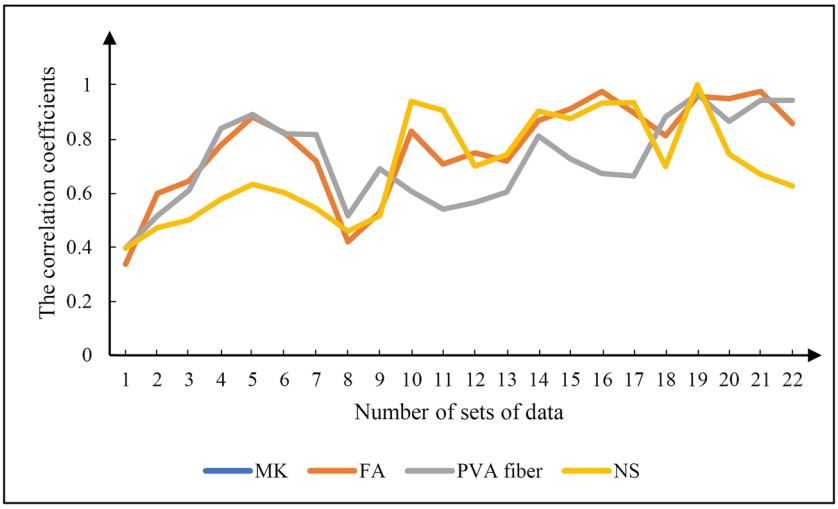

Figure 4: Correlation between each factor and quality loss rate.

loss rate, and compressive strength of nano-SiO_2 and PVA fiber-reinforced FMGM are more sensitive to nano-SiO_2 and PVA fiber doping. Analysis of the above data revealed that among these 22 sets of data, the correlation coefficients of both materials were higher when the nano-SiO_2 admixture was 1.0% and the PVA fiber admixture was 0.6%. Therefore, the mass loss rate, electric flux value, compressive strength loss rate, and compressive strength of nano-SiO_2 and PVA fiber-reinforced FMGM reached optimum values when the doping of PVA fibers was approximately 0.6% and the nano-SiO_2 dosage was approximately 1.0%, that is, the mechanical properties and durability performance of this material were optimal.

Finally, the gray correlation coefficients were averaged to determine the gray correlation between the four materials and the mass loss rate, electric flux value, compressive strength loss rate, and compressive strength of the nano-SiO_2 and PVA fiber-reinforced FMGM, and the results are listed in Table 8.

According to the results in Table 6, the effect of amount of the four materials on the compressive strength and mass loss rate is in the following decreasing order: MK and FA, PVA fiber, and nano-SiO_2. The effect of amount of doping of the four materials on the electric flux value and compressive strength loss rate is in the following decreasing order: MK and FA, nano-SiO_2, and PVA fiber. For the compressive strength and mass loss rate, the correlations of all 4 materials were greater than 0.6. For the electric flux values, the correlations of MK, FA, and nano-SiO_2 were greater than 0.6, while the

Table 8: Gray correlation degree of each comparison sequence and each reference sequence

Indicators	MK	FA	PVA fiber	NS
Compressive strength	0.9117	0.9117	0.6592	0.6438
Electric flux values	0.9607	0.9606	0.5961	0.6010
Loss rate of compressive strength	0.8360	0.8360	0.5869	0.5932
Mass loss rate	0.7695	0.7695	0.7218	0.6983

Table 9: Correlation coefficient between each factor and quality loss rate

Mix no.	MK	FA	PVA fiber	NS
1	0.3364	0.3364	0.3960	0.3960
2	0.5981	0.5981	0.5158	0.4719
3	0.6440	0.6440	0.6110	0.4999
4	0.7775	0.7775	0.8389	0.5768
5	0.8815	0.8815	0.8911	0.6322
6	0.8221	0.8221	0.8192	0.6010
7	0.7179	0.7179	0.8164	0.5434
8	0.4195	0.4195	0.5158	0.4582
9	0.5282	0.5282	0.6894	0.5160
10	0.8284	0.8284	0.6070	0.9384
11	0.7069	0.7069	0.5398	0.9056
12	0.7491	0.7490	0.5648	0.6993
13	0.7176	0.7177	0.6040	0.7414
14	0.8685	0.8686	0.8110	0.9036
15	0.9114	0.9113	0.7264	0.8757
16	0.9755	0.9756	0.6723	0.9327
17	0.8973	0.8973	0.6632	0.9348
18	0.8122	0.8122	0.8814	0.6981
19	0.9572	0.9573	0.9652	1.0000
20	0.9489	0.9489	0.8657	0.7437
21	0.9757	0.9757	0.9428	0.6693
22	0.8571	0.8570	0.9428	0.6257

correlations of PVA fiber were less than 0.6. For the compressive strength loss rate, only the correlations of the doping amounts of MK and FA were greater than 0.6; although the correlations of the 4 materials with each reference series were individually less than 0.6, they were close to 0.6. Therefore, the doping amounts of kaolin and FA, PVA fiber, and nano-SiO_2 have important effects on the mass loss rate, electric flux value, compressive strength loss rate, and compressive strength of the nano-SiO_2 and PVA fiber-reinforced FMGM. The results obtained in this study are consistent with the results of previous studies. Gray correlation analysis of (a) factors influencing the early frost resistance of structural concrete [48], (b) optimal mix ratio of multi-responsive recycled aggregate concrete [73], and (c) frost resistance index [74], produced similar results.

The results of the above analysis have a guiding effect on the ratio design of nano-SiO_2 and PVA fiber-reinforced FMGM. It has been proven that the gray correlation analysis method, having been applied in the fields of social, agricultural, and education systems and water quality assessment, has important practical value. Due to the small amount of data in this study, there will be a large error if regression analysis is adopted. To improve its mechanical properties and durability performance, the amount of nano-SiO_2 and PVA fiber admixture should be strictly controlled. When pre-configuring the geopolymer mortar, for optimal properties, the amount of PVA fiber admixture should be approximately 0.6%, and the amount of nano-SiO_2 admixture should be approximately 1.0%. At the same time, nano-SiO_2 should be taken with equal amounts of MK and FA according to the mass ratio of MK and FA.

5 Conclusion

In this study, the correlation coefficients of FA, MK, PVA fiber, and nano-SiO_2 admixtures, with mass loss rate under sulfate attack, electric flux value, compressive strength loss rate, and compressive strength of nano-SiO_2 and PVA fiber-reinforced FMGM were analyzed using gray correlation analysis. The degree of influence of the four materials on the compressive strength and durability of FMGM was determined as follows:

1) The durability and compressive strength of nano-SiO_2 and PVA fiber-reinforced FMGM are influenced by various factors with different sensitivities. The experimental results were validated using gray correlation analysis to clarify the relationships between the influencing factors. An important reference basis for the design and construction of nano-SiO_2 and PVA fiber-reinforced FMGM was obtained from the results of the analysis.
2) Using the gray system theory, the patterns of influence of the four materials' doping on the compressive strength and mass loss rate was in the following decreasing order: MK and FA, PVA fiber, and nano-SiO_2. The patterns of influence of the four materials' doping on the electric flux value and compressive strength loss rate are in the following decreasing order: MK and FA, nano-SiO_2, and PVA fiber. The results of this study are useful for guiding the preparation of geopolymer mortar.
3) The doping of all four materials, *i.e.*, MK and FA, PVA fiber, and nano-SiO_2, has important effects on the compressive strength and durability of the FMGM. The durability and compressive strength of the FMGM were optimized when the optimal dosage of PVA fibers was approximately 0.6% and the nano-SiO_2 dosage was approximately 1.0%. Therefore, to improve the mechanical properties and durability, the amount of FA and MK must be strictly controlled, with the amount of PVA fiber doping maintained at approximately 0.6% and the nano-SiO_2 dosage at approximately 1.0%.

Funding information: The authors would like to acknowledge the financial support received from Natural Science Foundation of Henan (Grant no. 212300410018), National Natural Science Foundation of China (Grant no. 51979251 and U2040224), Program for Innovative Research Team (in Science and Technology) in the University of Henan Province of China (Grant no. 20IRTSTHN009), and National Innovation and Entrepreneurship Training Program for College Students (Grant no. 202110459175).

Author contributions: All authors have accepted responsibility for the entire content of this manuscript and approved its submission.

Conflict of interest: The authors state no conflict of interest.

References

[1] Yang H, Zhang S, Lei W, Chen P, Shao D, Tang S, et al. High-ferrite Portland cement with slag: Hydration, microstructure, and resistance to sulfate attack at elevated temperature. Cem Concr Comp. 2022;130:104560.
[2] Golewski GL. Green concrete composite incorporating fly ash with high strength and fracture toughness. J Clean Prod. 2018;172:218–26.

[3] Ashish DK. Feasibility of waste marble powder in concrete as partial substitution of cement and sand amalgam for sustainable growth. J Build Eng. 2018;15:236–42.
[4] Wang L, Li G, Li X, Guo F, Lu X, Hanif A. Influence of reactivity and dosage of MgO expansive agent on shrinkage and crack resistance of face slab concrete. Cem Concr Comp. 2022;126:104333.
[5] Peng Y, Tang S, Huang J, Tang C, Liu Y. Fractal analysis on pore structure and modeling of hydration of magnesium phosphate cement paste. Fractal Fract. 2022;6:337.
[6] Guo XL, Xiong GY. Resistance of fiber-reinforced fly ash-steel slag based geopolymer mortar to sulfate attack and drying-wetting cycles. Constr Build Mater. 2021;269:121326.
[7] Zhang P, Kang L, Zheng Y, Zhang T, Zhang B. Influence of SiO_2/Na_2O molar ratio on mechanical properties and durability of metakaolin-fly ash blend alkali-activated sustainable mortar incorporating manufactured sand. J Mater Res Technol. 2022;18:3553–63.
[8] Shadnia R, Zhang LY, Li PW. Experimental study of geopolymer mortar with incorporated PCM. Constr Build Mater. 2015;84:95–102.
[9] Jindal BB. Investigations on the properties of geopolymer mortar and concrete with mineral admixtures: A review. Constr Build Mater. 2019;227:116644.
[10] Kan LL, Zhang L, Zhao YJ, Wu M. Properties of polyvinyl alcohol fiber reinforced fly ash based Engineered Geopolymer Composites with zeolite replacement. Constr Build Mater. 2020;231:117161.
[11] Han YC, Cui XM, Lv XS, Wang KT. Preparation and characterization of geopolymers based on a phosphoric-acid-activated electrolytic manganese dioxide residue. J Clean Prod. 2018;205:488–98.
[12] Han Q, Zhang P, Wu J, Jing Y, Zhang D, Zhang T. Comprehensive review of the properties of fly ash-based geopolymer with additive of nano-SiO_2. Nanotechnol Rev. 2022;11(1):1478–98.
[13] Shahmansouri AA, Bengar HA, Ghanbari S. Compressive strength prediction of eco-efficient GGBS-based geopolymer concrete using GEP method. J Build Eng. 2020;31:101326.
[14] Zhang SZ, Gong KC. Geopolymer. J Mater Sci Eng. 2003;21(3):430–6.
[15] Chithambaram SJ, Kumar S, Prasad MM. Thermo-mechanical characteristics of geopolymer mortar. Constr Build Mater. 2019;213:100–8.
[16] Zhu PH, Hua MQ, Liu H, Wang XJ, Chen CH. Interfacial evaluation of geopolymer mortar prepared with recycled geopolymer fine aggregates. Constr Build Mater. 2020;259:119849.
[17] Sreevidya V, Anuradha R, Venkatasubramani R. Strength study on fly ash-based geopolymer mortar. Asian J Chem. 2012;24(7):3255–6.
[18] Bingol S, Bilim C, Atis CD, Durak U. Durability properties of geopolymer mortars containing slag. IJST-T Civ Eng. 2020;44(1):561–9.
[19] Zhang P, Han X, Hu S, Wang J, Wang T. High-temperature behavior of polyvinyl alcohol fiber-reinforced metakaolin/fly ash-based geopolymer mortar. Compos Part B-Eng. 2022;244:110171.
[20] Zhang N, Yan CY, Li L, Khan M. Assessment of fiber factor for the fracture toughness of polyethylene fiber reinforced geopolymer. Constr Build Mater. 2022;319:126130.
[21] Korniejenko K, Lin WT, Simonova H. Mechanical properties of short polymer fiber-reinforced geopolymer composites. J Compos Sci. 2020;4(3):128.
[22] Abousnina R, Alsalmi HI, Manalo A, Allister RL, Alajarmeh O, Ferdous W, et al. Effect of short fibres in the mechanical properties of geopolymer mortar containing oil-contaminated sand. Polymers-Basel. 2021;13(17):3008.
[23] Li L, Sun HX, Zhang Y, Yu B. Surface cracking and fractal characteristics of bending fractured polypropylene fiber-reinforced geopolymer mortar. Fractal Fract. 2021;5(4):142.
[24] Zhang P, Zhang HS, Cui G, Yue XD, Guo JJ, David H. Effect of steel fiber on impact resistance and durability of concrete containing nano-SiO_2. Nanotechnol Rev. 2021;10(1):504–17.
[25] Ding Y, Bai YL. Fracture properties and softening curves of steel fiber-reinforced slag-based geopolymer mortar and concrete. Materials. 2018;11(8):1445.
[26] Abdollahnejad Z, Mastali M, Mastali M, Dalvand A. Comparative study on the effects of recycled glass-fiber on drying shrinkage rate and mechanical properties of the self-compacting mortar and fly ash-slag geopolymer mortar. J Mater Civ Eng. 2017;29(8):04017076.
[27] Zhang P, Wei S, Wu J, Zhang Y, ZHeng Y. Investigation of mechanical properties of PVA fiber-reinforced cementitious composites under the coupling effect of wet-thermal and chloride salt environment. Case Stud Constr Mat. 2022;17:e01325.
[28] Zhang P, Gao Z, Wang J, Guo J, Wang T. Influencing factors analysis and optimized prediction model for rheology and flowability of nano-SiO_2 and PVA fiber reinforced alkali-activated composites. J Clean Prod. 2022;366:132988.
[29] Wang L, Yu Z, Liu B, Zhao F, Jin M. Effects of fly ash dosage on shrinkage, crack resistance and fractal characteristics of face slab concrete. Fractal Fract. 2022;6:335.
[30] Du EX, Li HY. Experimental study on mechanical properties of PVA fiber reinforced high strength concrete. Agro Food Ind Hi-Tech. 2017;28(1):1099–103.
[31] Wang JQ, Dai QL, Si RZ, Guo SC. Investigation of properties and performances of Polyvinyl Alcohol (PVA) fiber-reinforced rubber concrete. Constr Build Mater. 2018;193:631–42.
[32] Kou SC, Poon CS. Properties of concrete prepared with PVA-impregnated recycled concrete aggregates. Cem Concr Comp. 2010;32(8):649–54.
[33] Ling Y, Zhang P, Wang J, Taylor P, Hu S. Effects of nanoparticles on engineering performance of cementitious composites reinforced with PVA fibers. Nanotechnol Rev. 2020;9(1):504–14.
[34] Zhang P, Li QF, Wang J, Shi Y, Ling YF. Effect of PVA fiber on durability of cementitious composite containing nano-SiO_2. Nanotechnol Rev. 2019;8(1):116–27.
[35] Givi AN, Rashid SA, Aziz FNA, Salleh MAM. Particle size effect on the permeability properties of nano-SiO_2 blended Portland cement concrete. J Comp Mater. 2011;45(11):1173–80.
[36] Zhang P, Yuan P, Guan J, Guo J. Fracture behavior of multi-scale nano-SiO_2 and polyvinyl alcohol fiber reinforced cementitious composites under the complex environments. Thero Appl Fract Mec. 2022;122:103584.
[37] Zheng Y, Zhuo J, Zhang Y, Zhang P. Mechanical properties and microstructure of nano-SiO2 and basalt-fiber-reinforced recycled aggregate concrete. Nanotechnol Rev. 2022;11(1):2169–89.

[38] Zhang P, Han Q, Wu J, Zhang Y. Mechanical properties of nano-SiO_2 reinforced engineered cementitious composites after exposure to high temperatures. Constr Build Mater. 2022;356:129123.
[39] Zhang P, Wang W, Lv Y, Wang K, Dai S. Effect of polymer coatings on the freezing–thawing and carbonation resistances of nano-SiO_2 and polyvinyl alcohol fiber-reinforced cementitious composites. J Mater Res Technol. 2022;21:69–83.
[40] Li GY. Properties of high-volume fly ash concrete incorporating nano-SiO_2. Cem Concr Res. 2004;34(6):1043–9.
[41] Xiao HG, Liu R, Zhang FL, Liu M, Li H. Role of nano-SiO_2 in improving the microstructure and impermeability of concrete with different aggregate gradations. Constr Build Mater. 2018;188:537–45.
[42] Bauer BJ, Liu DW, Jackson CL, Barnes JD. Epoxy/SiO_2 interpenetrating polymer networks. Polym Adv Technol. 1996;7(4):333–9.
[43] Huang Q, Shi XS, Wang QY, Tang L, Zhang HE. The influence of fiber on the resistance to chloride-ion penetration of concrete under the environment of carbonation. International Conference on Material Science and Application (ICMSA). Vol. 3. 2015. p. 223–38
[44] Feng QG, Yang Y, Yang LF, Chen Z, Zhu HY. Durability of high volume fly ash concrete with low water binder. J Wuhan Univ Technol. 2009;31(4):148–50.
[45] Castro S, Brito J. Evaluation of the durability of concrete made with crushed glass aggregates. J Clean Prod. 2013;41:7–14.
[46] Wen C, Zhang P, Wang J, Hu S. Influence of fibers on the mechanical properties and durability of ultra-high-performance concrete: A review. J Build Eng. 2022;52:104370.
[47] Chen SJ, Ren JX, Song YJ, Li Q. Salt freeze-thaw damage characteristics of concrete based on computed tomography. Vjesn. 2019;26(6):1753–63.
[48] Wang C. Gray correlation analysis of factors affect the ability of structure concrete in early antifreeze. Bull Chin Ceram Soc. 2015;34(11):3405–11.
[49] Nili M, Azarioon A, Hosseinian SM. Novel internal-deterioration model of concrete exposed to freeze-thaw cycles. J Mater Civ Eng. 2017;29(9):04017132.
[50] Sarkar M, Maiti M, Maiti S, Xu SL, Li QH. ZnO-SiO_2 nanohybrid decorated sustainable geopolymer retaining anti-biodeterioration activity with improved durability. Mat Sci Eng C-Mater. 2018;92:663–72.
[51] Xu F, Li H, Sun T, Zhou Y, Zhu J, Peng C, et al. Enhancing the mechanical and durability properties of fly ash-based geopolymer mortar modified by polyvinyl alcohol fibers and styrene butadiene rubber latex. Mater Express. 2021;11(9):1453–65.
[52] Abdollahnejad Z, Mastali M, Falah M, Shaad KM, Luukkonen T, Illikaninen M. Durability of the reinforced one-part alkali-activated slag mortars with different fibers. Waste Biomass Valori. 2021;12(1):487–501.
[53] Zhang P, Wei S, Zheng Y, Wang F, Hu S. Effect of single and synergistic reinforcement of PVA fiber and nano-SiO_2 on workability and compressive strength of geopolymer composites. Polymers. 2022;14(18):3765.
[54] Jin RY, Chen Q, Soboyejo ABO. Non-linear and mixed regression models in predicting sustainable concrete strength. Constr Build Mater. 2018;170:142–52.
[55] Tanyildizi H. Variance analysis of crack characteristics of structural lightweight concrete containing silica fume exposed to high temperature. Constr Build Mater. 2013;47:1154–9.
[56] Wang H, Zeng Z. Optimization of recycled high performance concrete base on principal component analysis. Concrete. 2011;4:51–3.
[57] Chen XP, Sun ZW, Pang JW. A research on durability degradation of mineral admixture concrete. Materials. 2021;14(7):1752.
[58] Chen K, Liang S, Zhang HT, Yang HS. Influence of parameters on mechanical properties of vibration-stirred water-stabilized gravel based on grey correlation analysis. Sci Technol Eng. 2019;12:1671–815.
[59] Deng JL. Figure on difference information space in grey relational analysis. J Grey Syst-UK. 2004;16(2):96–100.
[60] Zhu LH, Zhao C, Dai J. Prediction of compressive strength of recycled aggregate concrete based on gray correlation analysis. Constr Build Mater. 2021;273:121750.
[61] Deng JL. Relational space of grey systems. Fuzzy Mathematics. J Grey Syst-UK. 1985;4(2):1–10.
[62] Deng JL. Grey information space. J Grey Syst-UK. 1989;1(2):103–17.
[63] Jiang WQ, Shen XH, Xia J, Mao LX, Yang J, Liu QF. A numerical study on chloride diffusion in freeze-thaw affected concrete. Constr Build Mater. 2018;179:553–65.
[64] Zhou CH, Cao JZ, Chen ZP. Bond behavior of steel-recycled aggregate concrete interface after high temperatures and spraying water cooling. Front Mater. 2021;8:643510.
[65] Chou JS, Ongkowijoyo CS. Reliability-based decision making for selection of ready-mix concrete supply using stochastic superiority and inferiority ranking method. Reliab Eng Syst Safe. 2015;137:29–39.
[66] Liu JX, Liang BL. Grey correlation analysis of sensitive factors of concrete structures durability. Int Conf Adv Concr Struct. 2008;2:400–2.
[67] Lai WC, Chang TP, Wang JJ, Kan CW, Chen WW. An evaluation of Mahalanobis distance and grey relational analysis for crack pattern in concrete structures. Comp Mater Sci. 2012;65:115–21.
[68] Arici E, Kelestemur O. Optimization of mortars containing steel scale using Taguchi based grey relational analysis method. Constr Build Mater. 2019;214:232–41.
[69] Wang WC. Study on durability of nano-particles and fiber reinforced geopolymer mortar. Master's dissertation. Zhengzhou: Zhengzhou University; 2020.
[70] Xie NM, Liu SF. Research on evaluations of several grey relational models adapt to grey relational axioms. J Syst Eng Electron. 2009;20(2):304–9.
[71] Deng JL. Spread of grey relational space. J Grey Syst-UK. 1995;7(3):96–100.
[72] Deng JL. Grey group decision in grey rationale space. J Grey Syst-UK. 1998;10(3):177–82.
[73] Chang CY, Huang R, Lee PC, Weng TL. Determining the optimal mixture for recycled aggregate concrete with multiple responses. J Chin Inst Eng. 2014;37(2):165–74.
[74] Ye Y, Lu Q, Song H. Concrete durability in freezing-thawing circumstance using grey relation analysis. J Chin Three Gorges Univ (Nat Sci). 2015;37(1):18–21.